

UCSF

UC San Francisco Previously Published Works

Title

A hub-and-spoke circuit drives pheromone attraction and social behaviour in *C. elegans*

Permalink

<https://escholarship.org/uc/item/0zm5g3cn>

Journal

Nature, 458(7242)

ISSN

0028-0836

Authors

Macosko, Evan Z
Pokala, Navin
Feinberg, Evan H
[et al.](#)

Publication Date

2009-04-01

DOI

10.1038/nature07886

Peer reviewed



Published in final edited form as:

Nature. 2009 April 30; 458(7242): 1171–1175. doi:10.1038/nature07886.

A Hub-and-Spoke Circuit Drives Pheromone Attraction and Social Behavior in *C. elegans*

Evan Z. Macosko¹, Navin Pokala¹, Evan H. Feinberg¹, Sreekanth H. Chalasani¹, Rebecca A. Butcher², Jon Clardy², and Cornelia I. Bargmann¹

¹Howard Hughes Medical Institute, Laboratory of Neural Circuits and Behavior, The Rockefeller University, 1230 York Avenue, New York, NY 10065

²Department of Biological Chemistry and Molecular Pharmacology, Harvard Medical School, Boston, MA 02115

Abstract

Innate social behaviors emerge from neuronal circuits that interpret sensory information based on an individual's own genotype, sex, and experience. The regulated aggregation behavior of *C. elegans*, a simple animal with only 302 neurons, is an attractive system to analyze these circuits. Wild social strains of the nematode *Caenorhabditis elegans* aggregate in the presence of specific sensory cues, but solitary strains do not^{1,2,3,4}. Here we identify the RMG inter/motor neuron as the hub of a regulated circuit that controls aggregation and related behaviors. RMG is the central site of action of the neuropeptide receptor gene *npr-1*, which distinguishes solitary strains (high *npr-1* activity) from wild social strains (low *npr-1* activity); high RMG activity is essential for all aspects of social behavior. Anatomical gap junctions connect RMG to multiple classes of sensory neurons known to promote aggregation, and to ASK sensory neurons, which are implicated in male attraction to hermaphrodite pheromones⁵. We find that ASK neurons respond directly to pheromones, and that high RMG activity enhances ASK responses in social strains, causing hermaphrodite attraction to pheromones at concentrations that repel solitary hermaphrodites. The coordination of social behaviors by RMG suggests an anatomical hub-and-spoke model for sensory integration in aggregation, and points to functions for related circuit motifs in the *C. elegans* wiring diagram.

Many naturally-isolated social strains of *C. elegans* aggregate into feeding groups with dozens of animals, although other strains, including the laboratory strain N2, are solitary^{1,2}. Aggregating strains show several behavioral changes compared to solitary feeders: they accumulate on the border of a lawn of bacterial food (bordering) and move rapidly on food. Aggregation, bordering, and rapid movement are coordinately controlled by the neuropeptide Y receptor homologue NPR-12. Solitary strains have a high-activity form of NPR-1 (215-valine) whereas aggregating strains have a low-activity form of NPR-1 (215-

Users may view, print, copy, and download text and data-mine the content in such documents, for the purposes of academic research, subject always to the full Conditions of use:http://www.nature.com/authors/editorial_policies/license.html#terms

Author contributions

CIB is an Investigator of the Howard Hughes Medical Institute. EZM performed experiments; NP, EHF, SC, RAB, and JC developed experimental methods and reagents; EZM and CIB designed and interpreted experiments and wrote the paper.

phenylalanine); *npr-1* null mutants also aggregate^{2,6}. Neuropeptide control of aggregation provides an analogy to mammalian social behavior, which is regulated by the neuropeptides oxytocin and vasopressin⁷. In addition to genetic regulation by *npr-1*, aggregation is sensitive to environmental signals. It is stimulated by URX sensory neurons that detect environmental oxygen⁴, and ASH and ADL sensory neurons that sense noxious stimuli³. Attraction to low-oxygen environments promotes accumulation at the lawn border and feeding in groups, which have low oxygen levels compared to the open lawn^{4,8}. Population density, food availability³, and environmental stressors⁹ also modulate aggregation. The site of integration of these diverse cues is unknown.

How NPR-1 acts to regulate behavior is not well understood. A previous report using a genomic *npr-1* fragment identified the oxygen-sensing URX neuron as a site of *npr-1* action, but behavioral rescue was incomplete, with rescue of aggregation, partial rescue of bordering, and no rescue of rapid movement¹⁰. To identify additional neurons in which NPR-1 promotes solitary behavior, we first established that a full-length *npr-1* cDNA expressed from the endogenous *npr-1* promoter rescued solitary behavior in the strong loss of function mutant *npr-1(ad609lf)*, then refined the essential site of expression using other characterized promoters (Fig. 1a,b). Because promoter expression patterns in *C. elegans* can vary between transgenes, we used a bicistronic mRNA to express both *npr-1* and GFP, and identified GFP-positive neurons in each rescued line with solitary behavior (Supplementary Table 1 and Methods). Only promoters driving expression in the inter/motor neuron RMG showed robust rescue of aggregation, bordering, and locomotion speed (Fig. 1b and Supplementary Fig. 1).

We next asked whether RMG expression of *npr-1* is sufficient to suppress aggregation. No RMG-specific promoter is known, so an intersectional strategy was developed to drive *npr-1* expression only in cells that express both *flp-21* and *ncs-1*, using Cre-mediated recombination between LoxP sites that flanked transcriptional stop sequences. When *ncs-1::nCre* and *flp-21::LoxStopLox::GFP* strains were crossed together, the intersection between *ncs-1* and *flp-21* allowed strong and consistent GFP expression only in RMG and M2 pharyngeal neurons (Fig. 2a). We next inserted the *npr-1* cDNA into the *flp-21::LoxStopLox* plasmid (Fig. 2a); in *npr-1(lf)* animals expressing both *flp-21::LoxStopLox::npr-1* and *ncs-1::nCre*, aggregation, bordering, and high speed on food were strongly suppressed (Fig. 2b). M2 is synaptically isolated from neurons implicated in these behaviors, so we conclude that RMG expression of *npr-1* can block aggregation and related behaviors.

Mammalian neuropeptide Y receptors generally inhibit neurotransmitter release^{11,12}. To ask whether NPR-1 suppresses aggregation by inhibiting or by activating RMG, we killed RMG in wild-type and *npr-1(lf)* animals using a laser microbeam, anticipating an effect on the genotype(s) in which RMG is normally active. Killing RMG in *npr-1(lf)* eliminated aggregation, bordering, and rapid movement (Fig. 2c,d), whereas killing RMG in solitary wild-type animals had no effect (Fig. 2d). These results show that RMG neurons stimulate aggregation-related behaviors in *npr-1* mutants, and suggest that NPR-1 inhibits RMG activity in solitary strains.

Inspection of the *C. elegans* wiring diagram¹³ revealed that RMG is the hub of a gap junction network connecting seven classes of neurons, including the oxygen-sensitive URX neurons and the nociceptive ASH and ADL neurons previously implicated in aggregation behavior^{3,10} (Fig. 3a). RMG-ablated *npr-1* animals were normal in avoidance of high osmolarity, a behavior mediated by ASH¹⁴ (Supplementary Fig. 2). Therefore RMG is not essential for all functions of associated sensory neurons, but selectively required for aggregation and related behaviors.

Among the other neurons anatomically coupled to RMG, the ASK neurons were of particular interest. ASK is one of several neurons that integrate pheromone and food signals to regulate *C. elegans* development¹⁵, and it has recently been implicated in male attraction to hermaphrodite pheromones⁵. The role of ASK was probed using a *tax-4* mutation that affects sensory transduction: *tax-4* encodes a cyclic GMP-gated transduction channel expressed in ASK and other sensory neurons, but not in RMG¹⁶. *tax-4; npr-1(lf)* double mutants are strongly suppressed for aggregation and related behaviors¹⁰, and rescue of these behaviors requires *tax-4* expression in URX and an unknown sensory neuron¹⁰. We asked whether ASK might be the unknown neuron. Indeed, simultaneous expression of *tax-4* in URX and ASK resulted in near-complete rescue of aggregation and related behaviors in *tax-4; npr-1(lf)* double mutants (Fig. 3b). Rescue was also observed upon expression of *tax-4* in URX and ASJ neurons, which synapse onto ASK (Fig. 3b). Thus ASK and ASJ promote aggregation-related behaviors.

The connectivity of RMG suggests two models of behavioral output: 1) RMG could integrate sensory input through gap junctions and stimulate aggregation using its own chemical synapses; or 2) RMG could modify the output of associated sensory neurons, which all have chemical synapses. RMG is presynaptic to head muscles and interneurons that control forward and backward locomotion¹³ (Fig. 3a). To ask whether the synaptic output of RMG promotes aggregation, we used the Cre/Lox system to express the light chain of tetanus toxin (TeTx) in RMG of *npr-1(lf)* mutants. TeTx inhibits synaptic transmission by cleaving the synaptic vesicle protein synaptobrevin¹⁷. Aggregation and related behaviors were partially suppressed by TeTx expression in RMG (Fig. 3c). Co-expression of TeTx with a cleavage-resistant *C. elegans* synaptobrevin (Q68V) mutant¹⁷ significantly suppressed the RMG::TeTx effect, confirming that TeTx acts via synaptobrevin cleavage (Supplementary Fig. 3). Aggregation was also suppressed by expression of TeTx in ASK and ASJ, further implicating these neurons in aggregation behaviors, and TeTx expression in both RMG and ASK/ASJ had additive effects (Fig. 3c). Silencing or killing URX neurons suppresses aggregation^{10,18}, but TeTx expression in URX neurons had little effect unless the other neurons were silenced (Fig. 3c). These results suggest that synaptic outputs for aggregation are distributed, with contributions from both RMG and ASK/ASJ neurons.

We next asked whether activation of RMG or coupled neurons in solitary wild-type animals might induce aggregation. Neurons were activated by expressing a constitutively active protein kinase C homolog of *C. elegans* (*pkc-1(gf)*) that promotes synaptic transmission¹⁹ and neuropeptide release²⁰, and may have additional excitatory properties²¹. Expression of *pkc-1(gf)* in most RMG-coupled neurons elicited aggregation, bordering, and high speed in solitary strains, a near-complete transformation of their behavior (Fig. 3d). Expression in

subsets of neurons had partial effects suggesting contributions from RMG, URX, ASK/ASJ, and possibly other cells (Fig. 3d). Like the behavior of *npr-1(lf)* strains, *pkc-1(gf)*-induced behaviors were suppressed by killing RMG (Supplementary Fig. 3b). Thus simultaneous activation of RMG and sensory neurons by *pkc-1(gf)* can drive aggregation and related behaviors.

The dual involvement of ASK in aggregation and male attraction to hermaphrodites prompted an examination of pheromone responses in aggregating strains. A class of *C. elegans* pheromones termed ascarosides is attractive to males, but repulsive to solitary hermaphrodites, suggesting a role in sex-specific attraction for mating (Supplementary Fig. 4a)5,22. Ascarosides are constitutively secreted by *C. elegans*, providing a plausible aggregation signal23,24. Solitary wild-type hermaphrodites were repelled by ascarosides; by contrast, *npr-1(lf)* hermaphrodites were attracted to low levels of ascarosides, with responses resembling those of males (Fig. 4a,b). Expression of *npr-1* in RMG restored pheromone avoidance to *npr-1(lf)* hermaphrodites, linking this behavior to the RMG circuit (Fig. 4b).

Attraction to pheromones was absent in *tax-4; npr-1(lf)* double mutants, suggesting that *tax-4*-expressing sensory neurons detect ascarosides (Fig. 4c). Rescue of *tax-4* in ASK neurons restored ascaroside attraction to *tax-4; npr-1(lf)* strains, providing evidence that ASK is a relevant pheromone sensor (Fig. 4c). In a systematic analysis of the three pheromone components, a combination of C3 ascaroside with C6 or C9 drove synergistic attraction via ASK (Supplementary Fig. 4b,c). Developmental effects of ascarosides are also synergistic, and require higher pheromone concentrations than attraction, suggesting that attraction occurs at physiological pheromone levels24. Inhibiting synaptic transmission from ASK/ASJ or RMG neurons eliminated ascaroside attraction (Fig. 4d). The correlation between cells required for pheromone attraction and aggregation supports the hypothesis that these behaviors are functionally related.

Sensory properties of ASK were examined directly by monitoring sensory-evoked calcium transients with the genetically-encoded calcium indicator G-CaMP25. In both wild-type and *npr-1(lf)* animals, ASK responded to ascaroside cocktails (100 pM – 1 μ M) with a rapid diminution of fluorescence suggesting decreased calcium levels; fluorescence recovered upon ascaroside removal (Fig. 4e and Supplementary Fig. 4d). The rapid response in ASK neurons supports their identification as ascaroside-sensing neurons; the calcium decrease suggests that ASK uses a hyperpolarizing mode of sensory transduction26,27. At attractive nanomolar ascaroside concentrations, ASK calcium responses were reliably greater in *npr-1* animals than in wild type, with a greater calcium decrease upon ascaroside addition and a greater rebound following ascaroside removal (Fig. 4e,f).

To ask whether this apparent change in ASK activity could propagate across synapses, ascaroside responses were monitored in a synaptic target of ASK, the AIA interneuron. Ascaroside cocktails elicited increased G-CaMP fluorescence in AIA, suggesting depolarization (Fig. 4g); the average magnitude of this signal was significantly greater in *npr-1(lf)* than in wild-type animals (Supplementary Fig. 4e). The AIA response was diminished in *npr-1* animals whose ASK neurons were killed with a laser, suggesting that ASK sensory input is a major source of ascaroside signals to AIA (Fig. 4g,h). The inversion

of calcium signals (decrease in ASK, increase in AIA) suggests that ASK makes inhibitory synapses onto AIA. Ascaroside-induced AIA calcium signals were also diminished when the RMG neurons were killed (Fig. 4h). An RMG ASK double ablation resembled an ASK ablation alone, indicating that RMG and ASK affect AIA through a common process (Fig. 4g,h). The imaging results indicate that ASK senses ascarosides (along with other neurons), that the ASK response is propagated to downstream neurons, that RMG enhances ASK signaling, and that high *npr-1* activity diminishes it.

These results provide insight into behavioral mechanisms of aggregation, the anatomical circuit underlying the behavior, and the regulatory role of *npr-1*. Solitary animals ignore oxygen in the presence of food, and are repelled by ascarosides produced by other animals. In social *npr-1(lf)* animals, oxygen-sensing URX neurons promote accumulation at the lawn border, and ascaroside-sensing ASK neurons promote attraction to other animals (or neutralize repulsion). The altered pheromone response in *npr-1* hermaphrodites demonstrates that aggregation involves directed responses to other nematodes, not just a shared preference for low-oxygen environments. The analysis of RMG suggests a hub-and-spoke model for aggregation behavior, where distributed sensory inputs are coordinated through gap junctions with the RMG hub to produce distinct, distributed synaptic outputs. Mechanistically, calcium imaging suggests that RMG amplifies weak sensory signals in ASK to stimulate pheromone attraction. For example, the RMG circuit could depolarize ASK to increase tonic transmitter release at rest, and thereby increase the signal ASK sends when hyperpolarized by ascarosides.

In solitary strains, the neuropeptide receptor NPR-1 inhibits RMG function. In one model, NPR-1 might act by closing RMG gap junctions, gating access of sensory neurons to a shared circuit, but sparing their individual synaptic outputs. This instructive model for gap junction regulation is analogous to the dopaminergic regulation of gap junctions in the mammalian retina, where gap junctions link rod and cone visual pathways to increase light sensitivity at night; during the day, dopamine inhibits gap junctions to increase spectral and spatial resolution²⁸. Alternatively, NPR-1 could alter RMG excitability, and gap junctions could passively propagate this information from RMG to the sensory neurons to change their properties. In both models, *npr-1* shifts the properties of an entire anatomical circuit by modulating a single neuron. As RMG gap junctions are presently defined purely by anatomical criteria, further experiments are needed to determine whether RMG propagates electrical signals, calcium, cAMP, or other information.

Within the *C. elegans* wiring diagram, gap junction distributions are highly skewed. Most neurons have only a few gap junctions, but seventeen classes of neurons are gap junction hubs that link seven or more classes of neurons²⁹. We suggest that this circuit motif performs a characteristic computation wherever it appears.

Methods summary

Aggregation and bordering behaviors were measured essentially as described²; values report the average fraction of three or more behavioral assays of 150 animals each. Average

locomotion speed was calculated by tracking 20 animals for 10 minutes with an automated tracking system³⁰.

For RMG-selective expression of transgenes, LoxP-flanked *LacZ* sequence containing a transcriptional stop, three repeated polyA sequences, and two repeated mRNA cleavage sequences was inserted upstream of *npr-1::SL2::GFP* under the control of the *flp-21* promoter (*flp-21::LoxStopLox::cDNA(GFP, npr-1, TeTx, or pkc-1(gf))*). Transgenic animals containing this plasmid were crossed with animals expressing *nCre* under the *ncs-1* promoter (*ncs-1::nCre*). Strong and consistent expression was observed in RMG and M2; ADL, ASJ, and ASK were seen weakly and inconsistently.

For ascarioside chemotaxis assays, washed animals were placed in the center of a 4-quadrant plate with ascariosides in alternating quadrants, and scored after ten minutes. A chemotaxis index (C.I.) was calculated as (# of animals on pheromone quadrants – # of animals on buffer quadrants)/(total # of animals). In the cartoon in Fig. 4a, C.I. = –0.6. In Fig. 4 a cocktail of three ascariosides was used; individual ascariosides and other combinations are in Supplementary Fig. 4.

Calcium imaging of the AIA and ASK neurons was performed in a custom-fabricated microfluidic device, essentially as described²⁶. For ASK imaging, the transgene *kyEx2866* was used, with *GCaMP2.2b* (gift from Loren Looger) expressed under the *sra-9* promoter. For AIA imaging, the transgene *kyEx2916* was used, with *GCaMP2.2b* expressed under the T01A4.2 promoter. ASK fluorescence was recorded in the neuronal cell body, and AIA fluorescence was measured in the dorsal AIA process in the nerve ring.

Supplementary Material

Refer to Web version on PubMed Central for supplementary material.

Acknowledgements

We thank Loren Looger for GCaMP2.2b, Mike Nonet for cr-synaptobrevin, and Justin Ragains for synthesizing ascariosides. This work was funded by the Howard Hughes Medical Institute, the Harold and Leila Y Mathers Charitable Foundation, the Jensam Foundation, and NIH grants GM07739 (EZM and EHF), CA24487 (JC) and GM077943 (RAB).

References

1. Hodgkin J, Doniach T. Natural variation and copulatory plug formation in *Caenorhabditis elegans*. *Genetics*. 1997; 146:149–164. [PubMed: 9136008]
2. de Bono M, Bargmann CI. Natural variation in a neuropeptide Y receptor homolog modifies social behavior and food response in *C. elegans*. *Cell*. 1998; 94:679–689. [PubMed: 9741632]
3. de Bono M, Tobin DM, Davis MW, Avery L, Bargmann CI. Social feeding in *Caenorhabditis elegans* is induced by neurons that detect aversive stimuli. *Nature*. 2002; 419:899–903. [PubMed: 12410303]
4. Gray JM, et al. Oxygen sensation and social feeding mediated by a *C. elegans* guanylate cyclase homologue. *Nature*. 2004; 430:317–322. [PubMed: 15220933]
5. Srinivasan J, et al. A blend of small molecules regulates both mating and development in *Caenorhabditis elegans*. *Nature*. 2008; 454:1115–1118. [PubMed: 18650807]

6. Rogers C, et al. Inhibition of *Caenorhabditis elegans* social feeding by FMRFamide-related peptide activation of NPR-1. *Nat Neurosci.* 2003; 6:1178–1185. [PubMed: 14555955]
7. Hammock EA, Young LJ. Oxytocin, vasopressin and pair bonding: implications for autism. *Philosophical Transactions of the Royal Society of London (B).* 2006; 361:2187–2198.
8. Cheung BH, Cohen M, Rogers C, Albayram O, de Bono M. Experience-dependent modulation of *C. elegans* behavior by ambient oxygen. *Curr. Biol.* 2005; 15:905–917. [PubMed: 15916947]
9. Davies AG, Bettinger JC, Thiele TR, Judy ME, McIntire SL. Natural variation in the *npr-1* gene modifies ethanol responses of wild strains of *C. elegans*. *Neuron.* 2004; 42:731–743. [PubMed: 15182714]
10. Coates JC, de Bono M. Antagonistic pathways in neurons exposed to body fluid regulate social feeding in *Caenorhabditis elegans*. *Nature.* 2002; 419:925–929. [PubMed: 12410311]
11. Plummer MR, Rittenhouse A, Kanevsky M, Hess P. Neurotransmitter modulation of calcium channels in rat sympathetic neurons. *Journal of Neuroscience.* 1991; 11:2339–2348. [PubMed: 1678423]
12. Toth PT, Bindokas VP, Bleakman D, Colmers WF, Miller RJ. Mechanism of presynaptic inhibition of neuropeptide Y at sympathetic nerve terminals. *Nature.* 1993; 364:635–639. [PubMed: 8394510]
13. White JG, Southgate E, Thomson JN, Brenner S. The structure of the nervous system of *Caenorhabditis elegans*. *Philos Trans R Soc Lond B Biol Sci.* 1986; 314:1–340. [PubMed: 22462104]
14. Bargmann CI, Thomas JH, Horvitz HR. Chemosensory cell function in the behavior and development of *Caenorhabditis elegans*. *Cold Spring Harb Symp Quant Biol.* 1990; 55:529–538. [PubMed: 2132836]
15. Schackwitz WS, Inoue T, Thomas JH. Chemosensory neurons function in parallel to mediate a pheromone response in *C. elegans*. *Neuron.* 1996; 17:719–728. [PubMed: 8893028]
16. Komatsu H, Mori I, Rhee JS, Akaike N, Ohshima Y. Mutations in a cyclic nucleotide-gated channel lead to abnormal thermosensation and chemosensation in *C. elegans*. *Neuron.* 1996; 17:707–718. [PubMed: 8893027]
17. Schiavo G, et al. Tetanus and botulinum-B neurotoxins block neurotransmitter release by proteolytic cleavage of synaptobrevin. *Nature.* 1992; 359:832–835. [PubMed: 1331807]
18. Chang AJ, Chronis N, Karow DS, Marletta MA, Bargmann CI. A distributed chemosensory circuit for oxygen preference in *C. elegans*. *PLoS Biology.* 2006; 4:e274. [PubMed: 16903785]
19. Sieburth D, et al. Systematic analysis of genes required for synapse structure and function. *Nature.* 2005; 436:510–517. [PubMed: 16049479]
20. Sieburth D, Madison JM, Kaplan JM. PKC-1 regulates secretion of neuropeptides. *Nature Neuroscience.* 2007; 10:49–57. [PubMed: 17128266]
21. Okochi Y, Kimura KD, Ohta A, Mori I. Diverse regulation of sensory signaling by *C. elegans* nPKC-epsilon/eta TTX-4. *Embo J.* 2005; 24:2127–2137. [PubMed: 15920475]
22. White JQ, et al. The sensory circuitry for sexual attraction in *C. elegans* males. *Current Biology.* 2007; 17:1847–1857. [PubMed: 17964166]
23. Butcher RA, Fujita M, Schroeder FC, Clardy J. Small-molecule pheromones that control dauer development in *Caenorhabditis elegans*. *Nature Chemical Biology.* 2007; 3:420–422. [PubMed: 17558398]
24. Butcher RA, Ragains JR, Kim E, Clardy J. A potent dauer pheromone component in *Caenorhabditis elegans* acts synergistically with other components. *Proceedings of the National Academy of Sciences.* 2008; 105:14288–14292.
25. Nakai J, Ohkura M, Imoto K. A high signal-to-noise Ca(2+) probe composed of a single green fluorescent protein. *Nat. Biotechnol.* 2001; 19:137–141. [PubMed: 11175727]
26. Chalasani SH, et al. Dissecting a circuit for olfactory behaviour in *Caenorhabditis elegans*. *Nature.* 2007; 450:63–70. [PubMed: 17972877]
27. Suzuki H, et al. Functional asymmetry in *Caenorhabditis elegans* taste neurons and its computational role in chemotaxis. *Nature.* 2008; 454:114–117. [PubMed: 18596810]

28. Ribelayga C, Cao Y, Mangel SC. The circadian clock in the retina controls rod-cone coupling. *Neuron*. 2008; 59:790–801. [PubMed: 18786362]
29. Chen BL, Hall DH, Chklovskii DB. Wiring optimization can relate neuronal structure and function. *Proc Natl Acad Sci U S A*. 2006; 103:4723–4728. [PubMed: 16537428]
30. Ramot D, Johnson BE, Berry TL Jr, Carnell L, Goodman MB. The Parallel Worm Tracker: a platform for measuring average speed and drug-induced paralysis in nematodes. *PLoS ONE*. 2008; 3:e2208. [PubMed: 18493300]

Author Manuscript

Author Manuscript

Author Manuscript

Author Manuscript

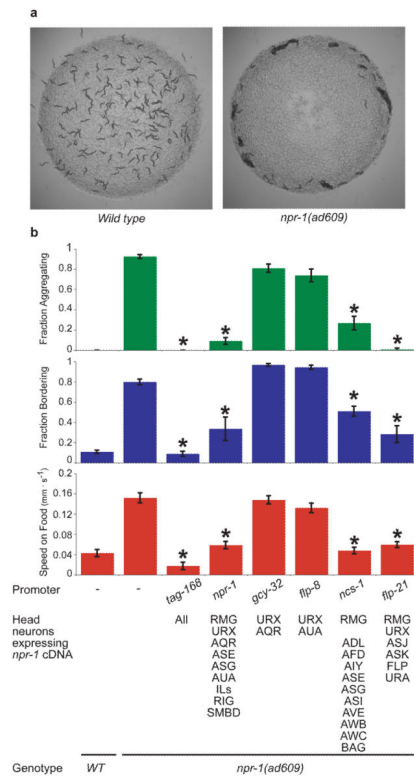


Figure 1. Selective expression of NPR-1 suppresses aggregation and related behaviors in *npr-1* mutants

a, Solitary behavior of 150 wild type N2 animals (left) and aggregation behavior of 150 *npr-1(ad609)* animals (right). **b**, Behavioral phenotypes of *npr-1(ad609)* animals expressing an *npr-1* cDNA under a pan-neuronal promoter (*tag-168*), its endogenous promoter (*npr-1*), URX promoters (*gcy-32* and *flp-8*) and RMG promoters (*ncs-1* and *flp-21*). For all figures, full promoter expression patterns are in Supplementary Table 1. Error bars indicate standard deviation (s.d.). Asterisk, different from *npr-1(ad609)* ($P < 0.01$, Bonferroni test).

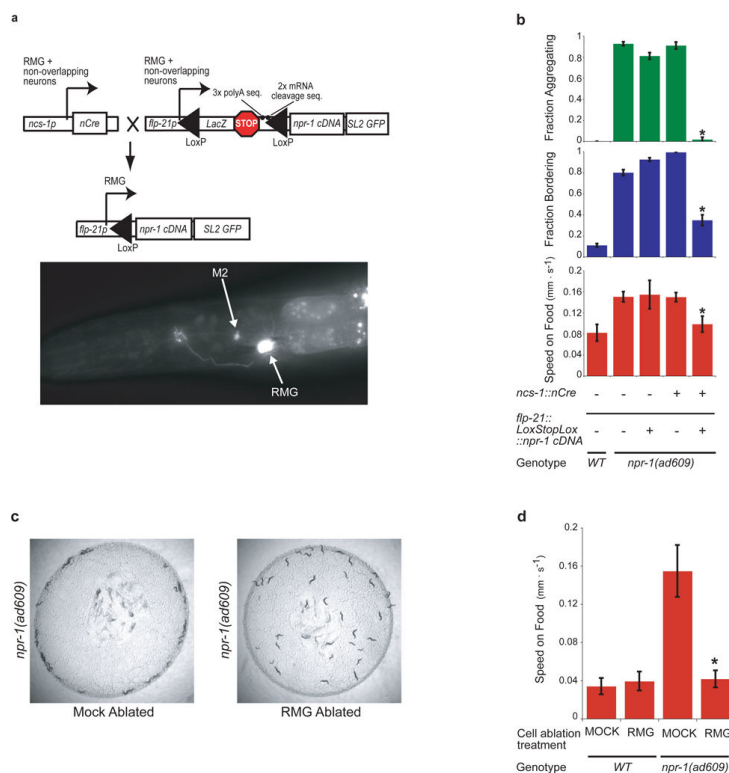


Figure 2. Inhibition of RMG by NPR-1 suppresses social behavior

a, Top, intersectional Cre/Lox strategy to express *npr-1* specifically in RMG. Bottom, L4 larva expressing *ncs-1::nCre* and *flp-21::LoxStopLox::GFP*. **b**, Aggregation and related behaviors of *npr-1(ad609)* animals carrying *ncs-1::nCre* and/or *flp-21::LoxStopLox::npr-1* transgenes. Asterisk, different from *npr-1(ad609)* ($P < 0.01$, Student's t-test). **c**, Mock-ablated or RMG-ablated *npr-1(ad609)* animals (mock-ablated: 97.1% bordering, 40% aggregating. RMG-ablated: 17% bordering, 0% aggregating. $\chi^2 = 43.05$, $P < 0.001$). **d**, Locomotion speed of WT and *npr-1(ad609)* animals, mock-ablated or RMG ablated. Asterisk, different from mock-ablated *npr-1(ad609)* ($P < 0.01$, Student's t-test). Error bars indicate s.d.

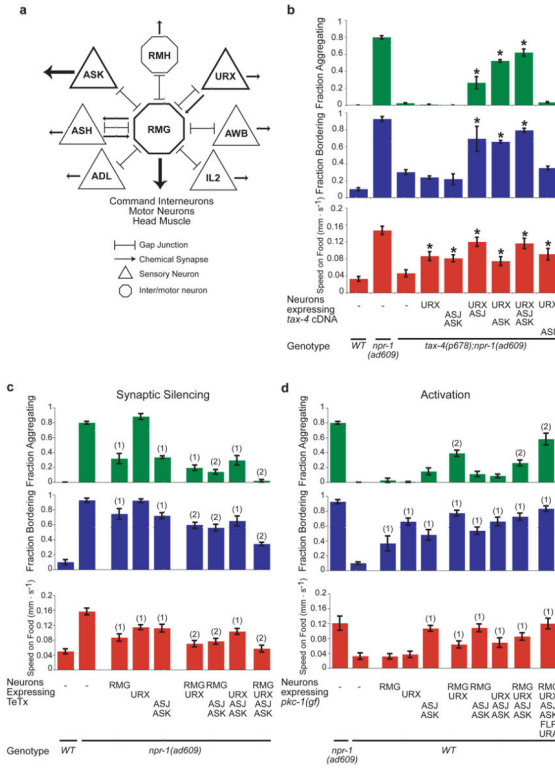


Figure 3. ASK and ASJ sensory neurons promote aggregation
a, Circuit diagram of neurons with gap junctions to RMG. RMG may also form gap junctions with RMF13. **b**, Rescue of aggregation and related behaviors in *tax-4(p678);npr-1(ad609)* animals expressing a *tax-4* cDNA. Asterisk, different from *tax-4;npr-1*. **c**, Aggregation and related behaviors of *npr-1(ad609)* animals expressing tetanus toxin light chain (TeTx). Statistics: different from ⁽¹⁾*npr-1(ad609)* ⁽²⁾*npr-1(ad609)* and overlapping single-transgene strains. **d**, Aggregation and related behaviors of wild-type animals expressing gain-of-function protein kinase C (*pkc-1(gf)*). Statistics: different from ⁽¹⁾WT ⁽²⁾WT and overlapping single-transgene strains. In b-d, P<0.01, Bonferroni test. Error bars indicate s.d.

Author Manuscript

Author Manuscript

Author Manuscript

Author Manuscript

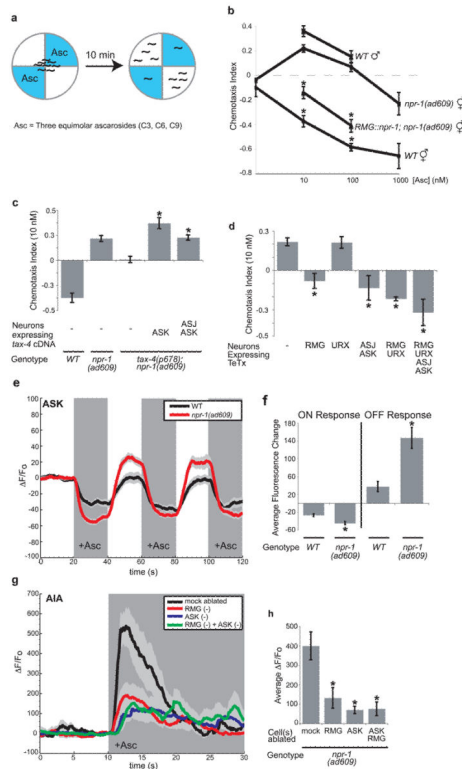


Figure 4. Behavioral and neuronal responses to pheromones

a, Diagram of pheromone chemotaxis assay. **b**, Ascaroside chemotaxis. Asterisk, different from *npr-1(ad609)*. **c**, ASK expression of *tax-4* restores pheromone attraction to *tax-4;npr-1*. Asterisk, different from *tax-4;npr-1*. **d**, TeTx expression in RMG or ASJ and ASK eliminates pheromone attraction in *npr-1(ad609)*. Asterisk, different from *npr-1(ad609)*. In b-d, $P < 0.01$, Bonferroni test. **e**, Ascaroside (100 nM) decreases G-CaMP calcium signals in ASK ($n = 17$ animals each). **f**, Average ASK fluorescence change to first ascaroside addition (ON) and removal (OFF). Asterisks, different from wild-type ($P < 0.01$, t-test). **g**, Ascaroside (1 μ M) induces G-CaMP calcium signals in AIA interneurons of *npr-1(ad609)*; for ablations, $n = 10$ animals; mock-ablated, $n = 16$. In e and g, dark shading indicates presence of ascarosides, light shading indicates standard error of the mean (s.e.m). **h**, Average AIA fluorescence change in 5s after ascaroside addition. Asterisk, different from mock-ablated ($P < 0.01$, Bonferroni test). In b-d, f and h, error bars indicate s.e.m.